

# Monte Carlo Simulation Study of a System with a Dielectric Boundary: Application to Calcium Channel Selectivity

DEZSŐ BODA<sup>a,\*</sup>, TIBOR VARGA<sup>a</sup>, DOUGLAS HENDERSON<sup>b</sup>, DAVID D. BUSATH<sup>c</sup>, WOLFGANG NONNER<sup>d</sup>, DIRK GILLESPIE<sup>d</sup> and BOB EISENBERG<sup>e</sup>

<sup>a</sup>Department of Physical Chemistry, University of Veszprém, H-8201, Veszprém PO Box 158, Hungary; <sup>b</sup>Department of Chemistry and Biochemistry, Brigham Young University, Provo, UT 84602-5700, USA; <sup>c</sup>Department of Physiology and Developmental Biology and Center for Neuroscience, Brigham Young University, Provo, UT 84602-5700, USA; <sup>d</sup>Department of Physiology and Biophysics, University of Miami School of Medicine, Miami, FL 33101, USA; <sup>e</sup>Department of Molecular Biophysics and Physiology, Rush Medical College, Chicago, IL 60612, USA

(Received October 2002; In final form January 2003)

Equilibrium Monte Carlo simulations are reported for a model of a biological calcium channel in which the region that includes the channel and the selectivity filter has a different dielectric coefficient than that of the bath. These regions are separated by a sharp dielectric boundary. This simple geometry makes it possible to use the image charge method to incorporate polarization effects. We also include a description of changes in solvation energy that arise when ions move between different dielectrics; we use the Born description of hydration with empirical ionic radii that yield experimental hydration energies. In calculations of  $\text{Ca}^{2+}$  vs.  $\text{Na}^{+}$  selectivity analogous to those of earlier work (Boda *et al.*, *Molec. Phys.*, 100, 2361 (2002)), we find that reducing the dielectric coefficient in the channel to values as low as 10 renders the channel model less calcium selective. Thus, this continuum description of polarization effects does not capture a delicate balance that seems to exist in biological channels between the energy that ions require for dehydration and the energy that ions gain by interaction with the charged groups in the pore.

**Keywords:** Polarization effect; Monte Carlo stimulation; Poisson's equation; Biological channel

## INTRODUCTION

Ion channels are large protein molecules that bridge the cell membrane by a hydrophilic pore. They make possible the controlled transfer of physiological ions

across the membrane and thus play a central role in many biological processes such as cell signaling, functioning of the nervous system and muscle contraction. Many drugs exert their actions on ion channels by blocking the passage of ions or by modifying the gating (the opening/closing mechanism) of the channel. Thus, ion channels are of great medical importance.

Besides gating, ionic selectivity is an essential feature of a large class of ion channels. Selectivity means that a channel allows only one type of physiological ion to pass, while it is rather impermeable for other physiological ions. Research on how the function of channels arises from their structure is a current topic of research that applies to the problem state-of-the-art results of several scientific fields such as molecular biology, biophysics, physical chemistry or statistical mechanics (for a recent review, see the work of Tieleman *et al.* [1] and references therein).

In several simulation studies [2–5] we have previously investigated the selectivity of calcium and sodium channels using a reductive model for the selectivity filter of the channel and a simple representation of the electrolyte based on the primitive model (PM). The filter is the interior of a cylinder that spans a membrane that excludes ions by hard walls. The specific structural features of each channel are represented by charged groups. In real channels these belong to amino acid side-chains that protrude into the bore of the filter, four negatively

\*Corresponding author. Tel.: +36-88-422-022/4424. Fax: +36-88-423-409. E-mail: boda@almos.vein.hu

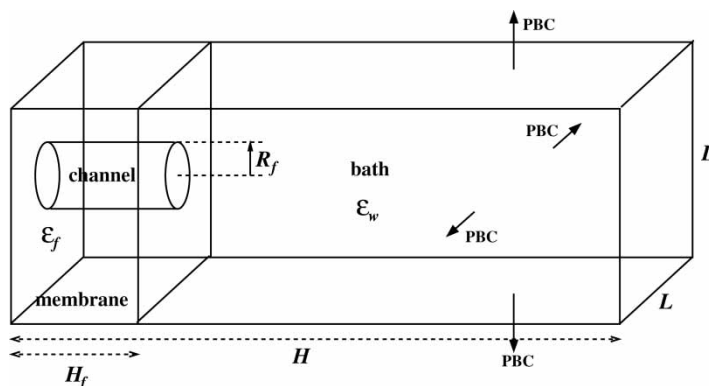


FIGURE 1 The simulation cell used in this work.

charged glutamate residues in Ca channels (EEEE locus), or aspartate, glutamate, lysine and alanine in Na channels (DEKA locus). In the model, these tethered groups are represented as charged spheres that are restricted to the filter but otherwise are free to move. In the PM of the electrolyte, ions are described as charged hard spheres, and water as an amorphous dielectric.

Whereas previous work with this model was based on a spatially uniform dielectric coefficient throughout the simulation cell, we now explore effects of dielectric non-uniformity. The simulation cell is divided into two regions that generally have different dielectric coefficients; one region contains the membrane and the channel, and the other region is a single bath. Because the system involves two half-spaces separated by a planar dielectric boundary, its electrostatics can be efficiently described using the method of image charges rather than a (more cumbersome) numerical solution of Poisson's equation. The singlet interaction of the ions with the dielectrics is described by combining the Born theory of hydration for bulk phases with a correction that accounts for the interaction with polarization charge induced in the dielectric boundary.

The long-range goal of this work is to develop a description of ion channel selectivity that is simple enough to compute while reproducing the essential observations. We test here a simple simulation system that includes different dielectrics in the membrane/channel and bath. Reducing the dielectric coefficient of the channel and membrane from 78.5 toward 10 in this system enhances the accumulation of ions in the channel while reducing the channel's preference for  $\text{Ca}^{2+}$  over  $\text{Na}^+$ . The latter effect seems to be due to the large energy of dehydration that is estimated from our ansatz for the singlet energies. It appears that a more accurate description of the solvent-ion interaction is needed to reproduce the strong  $\text{Ca}^{2+}$  selectivities seen in proteins including the Ca channel.

## METHODS

### The Model

The simulation cell used in this work (Fig. 1) is a simplification of a cell used in earlier simulations [4,5]. The purpose of this further simplification is to speed the computation of the electrostatics in the presence of different dielectrics. Instead of modeling two baths (one at each end of the channel) we remove the bath at one end of the channel and replace it by a hard wall. The dielectric coefficient in the half-space representing the bath ( $z > H_f$ ) is  $\epsilon_w = 78.5$ ; the other half-space, which includes the membrane and the channel, is assigned a parametric dielectric coefficient,  $\epsilon_f$ . This system involves a single, planar boundary between two dielectrics whose effects can be taken into account analytically. The simulation cell is rectangular (double layer geometry), confined between hard walls at  $z = 0$  and  $z = H$ , and periodic boundary conditions (PBC's) are applied in the  $x$  and  $y$  directions. The dimensions  $H$  and  $L$  are large enough so that a bulk-like electrolyte is obtained in the middle of the bath region. The ions are excluded from the membrane so that there are no ions in the region  $r > R_f - r_i$  and  $z < H_f + r_i$ . Here,  $r$  is the distance of the ion center from the axis of the channel, and  $r_i$  is the Pauling radius of ion  $i$  (see Table I for the ionic radii).

TABLE I The Pauling ionic radii, the Born-energies calculated using these radii, the experimental solvation energies and the Born-radii calculated from these values using the Born-equation (Eq. (5)) for the various ions

	$\text{Na}^+$	$\text{Ca}^{2+}$	$\text{Cl}^-$	$\text{O}^{-1/2}$
Pauling radii ( $r_i$ ) [ $\text{\AA}$ ]	0.95	0.99	1.81	1.4
Born-energy (Eq. (5)) [kJ/mole]	722	2771	379	-
Experimental solvation energy [kJ/mole]	424	1608	304	-
Born radii ( $R_i$ ) [ $\text{\AA}$ ]	1.62	1.71	2.26	-

*NVT* MC simulations are performed for the electrolyte in this simulation cell. Since the channel and the bath are subsystems of one simulation cell, they are in equilibrium. To accelerate equilibration between the small and high-density channel and the large and low-density bath, we use preference sampling as in earlier work [4]. The structural charges (the 8 oxygen atoms of the 4 carboxylates) in the filter are represented by 8 half-charged oxygen ions. They are restricted to the filter, so for their  $z$ -coordinate the condition  $z < H_f - r_O$  applies. Thus a net structural charge of  $-4e$  is located in the filter, which renders the channel cation selective.

The  $\text{Ca}^{2+}$  vs.  $\text{Na}^+$  selectivity is studied using the following procedure. We start from a 0.1M NaCl solution in the bath, and calculate the average number of  $\text{Na}^+$  ions absorbed in the channel. The binding affinity of the selectivity filter is characterized by this equilibrium absorption. Then we gradually add  $\text{CaCl}_2$  to the system while keeping the concentration of the  $\text{Na}^+$  ions constant at  $c_{\text{bath}}(\text{Na}^+) = 0.1\text{M}$ . Note that the concentration in the bath is an output of the simulation. To obtain a 0.1M  $\text{Na}^+$  concentration, we perform a short simulation to estimate the  $\text{Na}^+$  concentration established in the bath; the cell width is then adjusted to achieve a  $\text{Na}^+$  concentration closer to the desired value. As the proportion of  $\text{Ca}^{2+}$  ions in the system increases, the calcium ions drive out sodium ions from the filter according to the CSC (charge space competition) mechanism [2,6]: the channel is selective for  $\text{Ca}^{2+}$  because one  $\text{Ca}^{2+}$  provides twice the charge for the neutralization of the oxygen ions while occupying about the same volume as a  $\text{Na}^+$  ion. The crucial question is whether this selectivity occurs at  $\text{Ca}^{2+}$  bath concentrations as low as those found in the biological channel ( $\sim 1\ \mu\text{M}$ ).

Further details of our simulation method can be found in Refs. [2–5]. The length of the cell is set to  $H = 750\ \text{\AA}$ , while the width of the cell is varied in the range  $L = 50\text{--}100\ \text{\AA}$  with a resulting variation in the number of sodium ions in the system (100–400) to keep the  $\text{Na}^+$  concentration in the bath constant. Large system sizes are necessary because, at low  $\text{Ca}^{2+}$  ion concentrations, the  $\text{Ca}^{2+}$  concentration can be further reduced only by increasing the system size since the number of  $\text{Ca}^{2+}$  ions cannot fall below one. The length and the radius of the channel are  $H_f = 10\ \text{\AA}$  and  $R_f = 5\ \text{\AA}$ , respectively, as in previous work [4]. The length of the simulation is 2, 3, 3.6 and 5.2 million MC cycles for  $\epsilon_f = 78.5, 40, 20$  and 10, respectively. For lower  $\epsilon_f$  the sampling is poorer because of the deep energy well produced by the less-screened interaction of a cation with the oxygen ions. In these cases, longer simulations are necessary. In one MC cycle repositioning of each particle is attempted at least once. The particle to be moved is selected randomly. The MC move can be a usual

particle displacement, a jump (by which the particle is randomly displaced to a location somewhere in the whole simulation cell), or a particle exchange between the bath and the filter [4]. This particle exchange is a biased move allowing a preference sampling for the accelerated equilibration between the bath and the filter (details can be found in Ref. [4]). This preference sampling is useful even in computations with  $\epsilon_f = 78.5$ .

The long range corrections resulting from the periodic images in  $x$  and  $y$  directions, where PBCs are applied, are ignored. We have checked whether the results depend on the  $L$  dimension by performing simulations for the same bath concentrations with various system sizes and found that the results do not depend appreciably on system size; thus the dimensions given above can be used.

### The ion–ion Interaction Energy

The pairwise ion–ion interaction energy must be computed in a manner that ensures that Poisson’s equation is always obeyed. Poisson’s equation in situations with non-uniform dielectrics can usually only be solved numerically. Our simulation involves a situation in which an analytical solution can be obtained: space is divided into two half spaces with two different dielectric coefficients ( $\epsilon_f$  and  $\epsilon_w$ ) and a sharp, planar dielectric boundary at  $z = H_f$ . An ion will induce a surface charge at this boundary, and the interaction of the ion with this polarization charge can be taken into account by the image charge method. An ion of charge  $q$  at a distance  $d$  from the boundary produces an electrical potential at the point  $P$ . If this point is on the same side as the charge (Fig. 2a), the potential is

$$\Phi(P) = \frac{1}{4\pi\epsilon_0\epsilon_{\text{same}}} \left( \frac{q}{R_1} - \frac{\theta q}{R_2} \right), \quad (1)$$

where

$$\theta = \frac{\epsilon_{\text{other}} - \epsilon_{\text{same}}}{\epsilon_{\text{other}} + \epsilon_{\text{same}}}, \quad (2)$$

and  $\epsilon_{\text{same}}$  and  $\epsilon_{\text{other}}$  are, respectively, the dielectric coefficients on the same and other side as the ion. If the point  $P$  is on the opposite side as the ion (Fig. 2b), the potential is given as

$$\Phi(P) = \frac{1}{2\pi\epsilon_0(\epsilon_{\text{same}} + \epsilon_{\text{other}})} \frac{q}{R_1}. \quad (3)$$

The interaction energy between an ion  $q$  and another ion  $q'$  at the point  $P$  is

$$E^C = q'\Phi, \quad (4)$$

where the superscript  $C$  refers to Coulombic interaction. Furthermore, due to the hard core, the energy is infinite if the distance of ions  $i$  and  $j$  is less

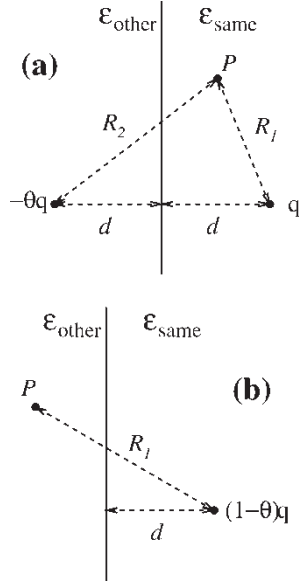


FIGURE 2 Charges and image charges when the probe point  $P$  is on the same (a) and the opposite (b) side as the source charge.

than  $r_i + r_j$ . The described Coulombic energy is a pair energy because it involves the interaction between two ions. Furthermore, there is an energy that involved the interaction of each individual ion with its own polarization charge, and hence is a singlet energy.

### The Singlet Energy

The singlet energy is the electrostatic work necessary to move an ion from a position far in a vacuum to its position in the dielectric of the simulation cell. If the simulation cell contains a uniform bulk dielectric, this work can be estimated as the Born energy [7].

$$E^B = -\frac{q^2}{8\pi\epsilon_0 R} \left(1 - \frac{1}{\epsilon}\right), \quad (5)$$

where  $R$  is the radius of the ion. It is well known that with ions assigned their Pauling radii (Table I), the Born equation overestimates the experimental values for the hydration energy (calculated by using  $\epsilon = \epsilon_w$ ). Table I gives these calculated energies, as well as the experimental values. For a better representation of the experimental hydration energies, we use adjusted ionic radii in the Born equation that are larger than the Pauling radii (see Table I). Note that these radii are used only in the computation of the singlet energy; ion pair interactions are computed using the Pauling radii. Using the empirical Born radii, the difference between an ion's singlet energy far to the left ( $\epsilon_f$ ) and to the right

( $\epsilon_w$ ) of the boundary is

$$\Delta E_i^s = \frac{q_i^2}{8\pi\epsilon_0 R_i} \left(\frac{1}{\epsilon_f} - \frac{1}{\epsilon_w}\right). \quad (6)$$

This energy is positive for an ion moving from the bath into the channel.

In our simulations, ions are within a finite distance from a dielectric boundary. Thus, in addition to the bulk singlet energy, we have to add the ion's interaction with the charge that the ion induces at the boundary (or, equivalently, the ion's interaction with its image charge). From Eqs. (1)–(6), if the ion center is in the region  $|z - H_f| > R_i$  the total singlet energy is [8]

$$E_i^s(z) = \Delta E_i^s - \frac{q_i^2 \theta}{16\pi\epsilon_0 \epsilon_f z - H_f}, \quad \text{if } z < H_f - R_i \quad (7)$$

$$E_i^s(z) = -\frac{q_i^2 \theta}{16\pi\epsilon_0 \epsilon_w z - H_f}, \quad \text{if } H_f + R_i < z$$

with

$$\theta = \frac{\epsilon_f - \epsilon_w}{\epsilon_f + \epsilon_w}. \quad (8)$$

For the region  $H_f - R_i < z < H_f + R_i$ , we use a simple interpolation between the singlet energies that apply to the edges of this region. Specifically, the tangents of the curves describing the singlet energies in the regions  $H_f - r_i < z < H_f$  and  $H_f < z < H_f + r_i$  are extrapolated in each half space to the boundary. This yields a unique singlet energy at the boundary whose variation with  $z$  has a discontinuity in its derivative (see Fig. 3). The specific interpolation formulae are

$$E_i^s(z) = E_i^s(0) + \frac{q_i^2 \theta}{16\pi\epsilon_0 \epsilon_f R_i^2} (z - H_f), \quad \text{if } H_f - R_i < z < H_f \quad (9)$$

$$E_i^s(z) = E_i^s(0) + \frac{q_i^2 \theta}{16\pi\epsilon_0 \epsilon_w R_i^2} (z - H_f), \quad \text{if } H_f < z < H_f + R_i$$

where

$$E_i^s(0) = \Delta E_i^s + \frac{q_i^2 \theta}{8\pi\epsilon_0 \epsilon_f R_i} = -\frac{q_i^2 \theta}{8\pi\epsilon_0 \epsilon_w R_i} \quad (10)$$

is the value of  $E_i^s$  at the dielectric boundary (at the vertical line at  $z = H_f$  in Fig. 3).

## RESULTS AND DISCUSSION

First, we compare simulation results from the model with one bath (Fig. 1) to the previously used two-bath model [4], to see if the further simplification of

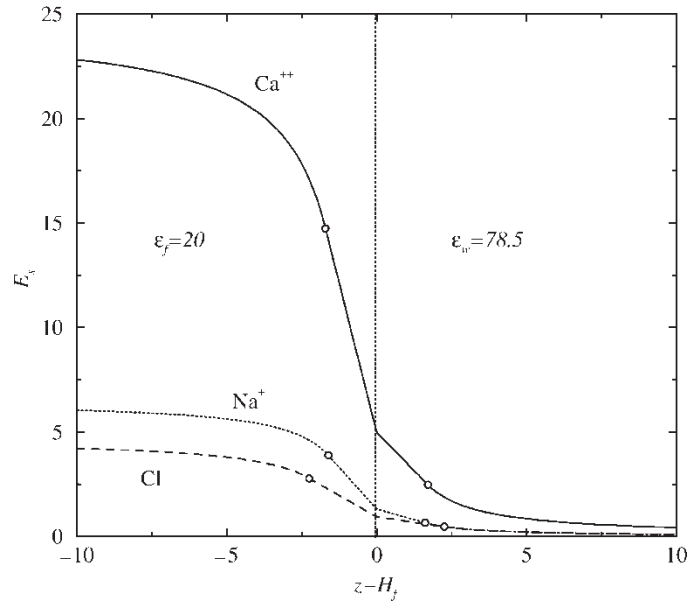


FIGURE 3 The singlet energy as a function of  $z - H_f$  for various ions when  $\epsilon_f = 20$  and  $\epsilon_w = 78.5$ . The open circles denote the positions  $-R_i$  and  $R_i$ .

the model has substantial effects on the accumulation of ions in the channel. With a uniform dielectric coefficient ( $\epsilon_f = \epsilon_w = 78.5$ ) we find that the channel in the one-bath model accumulates a larger number of counterions than the channel with two baths (Fig. 4). This result is expected, given that structural charges in the channel are less well screened by only one bath than by two. This finding conforms with earlier results obtained in simulations with a channel of infinite length [2,3], as compared to

simulations with a channel of finite length that connects two baths [4,5]. Regarding the  $\text{Ca}^{2+}$  vs.  $\text{Na}^+$  selectivity we note that the channel with one bath requires only slightly higher  $\text{Ca}^{2+}$  concentration in the bath in order to substitute half on the  $\text{Na}^+$  in the channel by  $\text{Ca}^{2+}$ . Thus this essential channel property is not substantially altered when one of the baths is omitted from the system.

Density profiles for one-bath simulations with uniform dielectric coefficient (78.5) are shown in

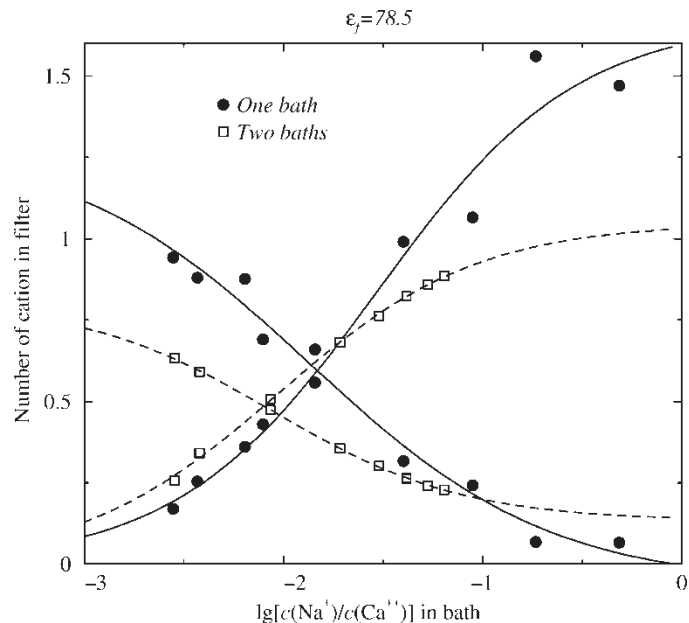


FIGURE 4 Comparison of the selectivity curves obtained from the one-bath geometry [4] and the two-bath geometry (present work) when the dielectric coefficient is 78.5 everywhere. The decreasing and increasing curves apply to sodium and calcium ions, respectively.

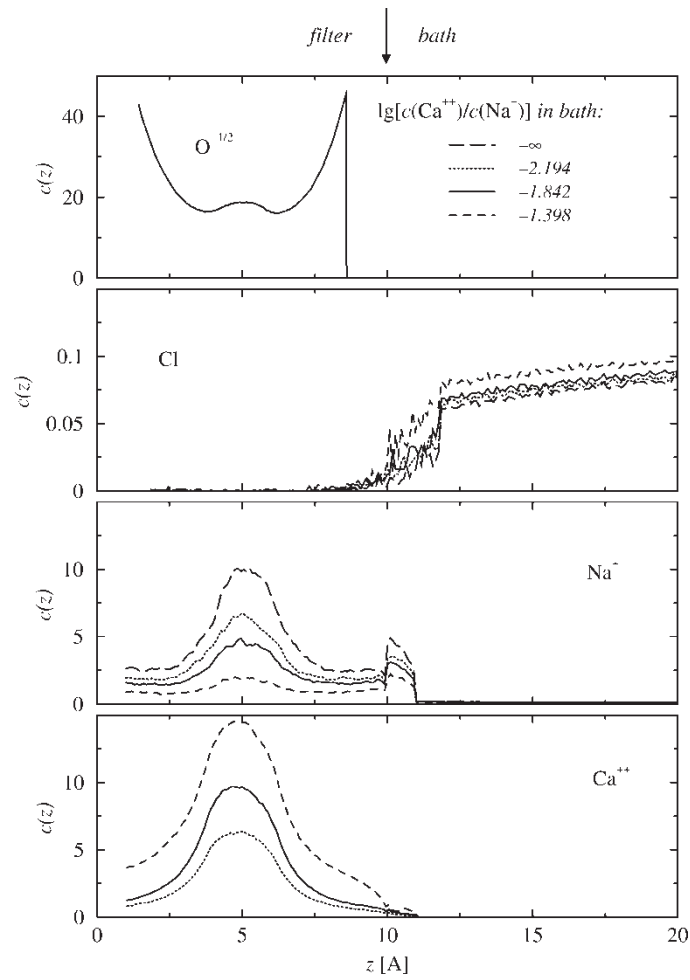


FIGURE 5 Axial profiles of molar concentration for various calcium concentrations in the bath (dielectric coefficient is 78.5 everywhere).

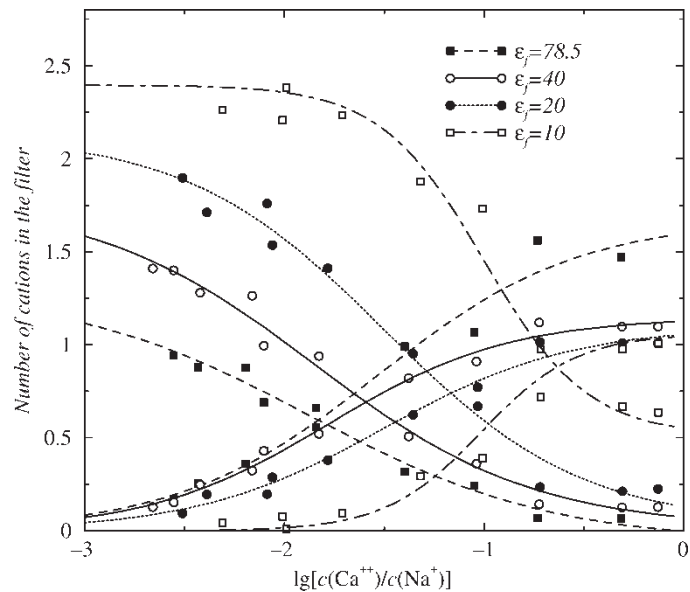


FIGURE 6 Sodium vs. calcium selectivity curves obtained for various values of  $\epsilon_f$  in the one-bath geometry. The decreasing and increasing curves apply to sodium and calcium ions, respectively.



Fig. 5. Profiles for other values of the dielectric coefficient  $\epsilon_f$  are qualitatively similar to these, and are not shown. These profiles reflect the influence of the hard wall confining the simulation cell at  $z = 0$ . An interfacial layer is found near this wall with an excess of oxygen ions. Cations tend to accumulate in the middle of the filter. Overall, the profiles are quite similar to those found in the two-bath geometry (Fig. 7 in Ref. [4]). It appears that the one-bath geometry gives results that are reasonably similar to results obtained with the more realistic two-bath geometry. This justifies the use of a simpler geometry, which greatly reduces computation times in exploring effects of non-uniform dielectrics (or solvation) in this system.

Figure 6 shows accumulated simulation results obtained with dielectric coefficients in the channel varied between 78.5 and 10. Reducing the dielectric coefficient in the channel produces a stronger accumulation of  $\text{Na}^+$  into the channel, such that local electroneutrality becomes more closely maintained (the electroneutral channel would contain 4  $\text{Na}^+$  or 2  $\text{Ca}^{2+}$ ). By contrast, accumulation of  $\text{Ca}^{2+}$  is reduced as the dielectric coefficient in the channel is made smaller.

From calcium block of sodium currents, biological calcium channels appear to be occupied about one-half of the time by  $\text{Ca}^{2+}$  when 1  $\mu\text{M}$   $\text{Ca}^{2+}$  and 0.1 M  $\text{Na}^+$  are present in the bath. Compared to this experimental observation, the previous uniform dielectric model [4] gives a smaller affinity for  $\text{Ca}^{2+}$  by about two orders of magnitude. In the current simulations,  $\text{Ca}^{2+}$  affinity declines another order of magnitude as the dielectric coefficient in the channel is reduced to 10. Evidently, with a low dielectric in the channel, the singlet energy inhibits  $\text{Ca}^{2+}$  entry into the channel more than increased ion-ion interactions with the confined oxygens enhance it. Perhaps additional mechanisms increase absorption selectivity in biological channels. For instance, it may be that the carboxylate anions of the EEEE locus cannot be adequately represented by two unconnected half-charged oxygen ions per carboxylate group, as has been suggested by recent simulations with model channels having complete glutamate side chains [10].

However, we also wish to draw attention to the fine balance between dehydration and coordination inherent in these calculations.  $\text{Ca}^{2+}$  and  $\text{Na}^+$  have very similar crystal radii (Table I), but differ in their valences. Since hydration energies vary in proportion to the square of the valence, any error in estimating the diameter dependence of the hydration energy would affect the value for  $\text{Ca}^{2+}$  four times more strongly than the value for  $\text{Na}^+$ . From our simulation results we might suspect that our formulation overestimates the singlet energies for small dielectric coefficients. It is instructive to

consider a more detailed model of ion-solvent interaction, for instance, the analytically solvable MSA model of ions in a dipolar hard-sphere solvent [9]. The ion-dipole interaction energy in this system can be expressed in the form of the Born equation, but with the ionic radius replaced by the effective radius

$$R = r_i + \frac{r_s}{\lambda}, \quad (11)$$

where  $r_s$  and  $r_i$  are the solvent and ion radii, and  $\lambda$  is a function of the dielectric coefficient that results from the orientational polarization of the solvent dipoles:

$$\lambda^2(1 + \lambda)^4 = 16\epsilon \quad (12)$$

For  $\epsilon$  varying between 78.5 and 10,  $\lambda$  varies between 2.65 and 1.72 and the effective radii that apply to  $\text{Ca}^{2+}$  or  $\text{Na}^+$  increase about 1.2-fold. The bulk solvation energies computed from Eq. (11) for  $\epsilon = 10$  are 1.2 times smaller in magnitude than those that would be computed using the Born radii that give appropriate hydration energies for  $\text{Ca}^{2+}$  or  $\text{Na}^+$  at  $\epsilon = 78.5$ . In this ion-dipole model of solvation,  $\text{Ca}^{2+}$  would be accumulated even less than in the model that we have simulated. On the other hand, the example shows that a more detailed model of the solvent can give results that differ substantially from the continuum model of hydration that we use in our present simulations. More accurate treatments of solvation thus seem necessary and should be pursued in the future.

### Acknowledgements

This work was supported by grants from the Hungarian National Research Fund (OTKA-F035222, to D.B.), DARPA (B.E., W.N.), NIH (AI 23007, to D.D.B. and T32NS07044 to DG) and NSF (CHE98-13729, to D.H.). The authors thank the organizers of the Yangtze Conference on Fluids and Interfaces where an inspiring environment was available for discussions of this work.

### References

- [1] Tieleman, D.P., Biggin, P.C., Smith, G.S. and Sansom, M.S.P. (2001) "Simulation approaches to ion channel structure-function relationships", *Quart. Rev. Biophys.* **34**, 473.
- [2] Boda, D., Busath, D.D., Henderson, D. and Sokolowski, S. (2000) "Monte Carlo simulations of the mechanism for channel selectivity: the competition between volume exclusion and charge neutrality", *J. Phys. Chem. B* **104**, 8903.
- [3] Boda, D., Henderson, D. and Busath, D.D. (2001) "Monte Carlo study of the effect of ion and channel size on the selectivity of a model calcium channel", *J. Phys. Chem. B* **105**, 11574.
- [4] Boda, D., Henderson, D. and Busath, D.D. (2002) "Monte Carlo study of the selectivity of calcium channels: improved geometrical model", *Mol. Phys.* **100**, 2361.

- [5] Boda, D., Busath, D.D., Eisenberg, B., Henderson, D. and Nonner, W. (2002) "Monte Carlo simulations of ion selectivity in a biological Na channel: Charge-space competition", *Phys. Chem. Chem. Phys.* **4**, 5154.
- [6] Nonner, W., Catacuzzeno, L. and Eisenberg, B. (2000) "Binding and selectivity in L-type calcium channels: a mean spherical approximation", *Biophys. J.* **79**, 1976.
- [7] Born, M. (1920) "Volumen und hydrationswärme der ionen", *Z. Phys.* **1**, 45.
- [8] Neumcke, B. and Läuger, P. (1969) "Nonlinear electrical effects in lipid bilayer membranes, II. Integration of the generalized Nernst-Planck equation", *Biophys. J.* **9**, 1160.
- [9] Garisto, F., Kusalik, P.G. and Patey, G.N. (1983) "Solvation energy of ions in dipolar solvents", *J. Chem. Phys.* **79**, 6294.
- [10] Ramakrishnan, V. (2002) *Molecular Computations on Selectivity and Permeation in Ion Channels and Transporters* (Doctoral Dissertation, Brigham Young University, Provo, UT).